



Institute for

Shock Physics

WASHINGTON STATE UNIVERSITY

“Shock Compression Response of an Insensitive High Explosive Single Crystal: 1, 1-Diamino-2, 2-Dinitroethene (FOX-7)”

J. M. Winey, Y. Toyoda, and Y. M. Gupta

DOI: 10.1063/1.5140194

Published: April 2020

Journal of Applied Physics

Shock compression response of an insensitive high explosive single crystal: 1,1-diamino-2,2-dinitroethene (FOX-7)

J. M. Winey,^{1,*} Y. Toyoda¹ and Y. M. Gupta^{1,2}

¹*Institute for Shock Physics, Washington State University, Pullman, WA 99164-2816, USA*

²*Department of Physics, Washington State University, Pullman, WA 99164-2816, USA*

Abstract:

Insensitive high explosives (IHEs) – that do not compromise performance – are of considerable interest as a safer alternative to conventional high explosives, such as pentaerythritol tetranitrate (PETN) and cyclotrimethylenetrinitramine (RDX). Despite the strong interest in using IHEs, shock compression experiments on IHE single crystals have not been reported. To address this need, plate impact experiments were conducted to measure wave profiles in 1,1-diamino-2,2-dinitroethene (FOX-7) single crystals – a representative IHE crystal – shocked to 21 GPa longitudinal stress. Particle velocity histories, measured using laser interferometry, show a clear two-wave structure (elastic-inelastic response) at modest stresses (<3.8 GPa). Wave profiles at higher stresses show a single (overdriven) wave. Measured shock velocities and wave profiles provide accurate Hugoniot data to 21 GPa. The measured wave profiles to 21 GPa show no sign of energy release due to chemical decomposition and constitute the first demonstration of an IHE single crystal insensitivity under plane shock compression. Numerical simulations using a phenomenological material model developed for FOX-7 showed good agreement with the measured wave profiles. The experimental findings and continuum simulations presented here constitute a significant first step in gaining insight into the shock compression response of IHE single crystals.

*Corresponding author email: mwiney@wsu.edu

I. INTRODUCTION

High performance and low sensitivity to shock initiation are two key desirable attributes for high explosives (HEs).¹ In recent years, insensitive high explosives (IHEs) have received significant attention as an alternative to conventional HEs, such as pentaerythritol tetranitrate (PETN) and cyclotrimethylenetrinitramine (RDX), to provide lower sensitivity without compromising high performance. Despite the strong interest in using IHE crystals, the shock compression response of these crystals has received little attention. In particular, a fundamental unanswered question is: Why are IHE crystals insensitive to shock initiation? To address such fundamental questions, experimental shock wave studies on well-oriented IHE single crystals constitute an important scientific need because they avoid the complexities inherent to the shock response of composite (or plastic-bonded) explosives, providing insight into the intrinsic response of IHE crystals incorporated into composite HE formulations. In contrast to the significant experimental studies that have been carried out on shock-compressed conventional HE single crystals,²⁻⁹ well characterized experiments to examine the shock response of IHE single crystals have not been reported to date.

To address this need, we report here on the shock compression response of 1,1-diamino-2,2-dinitroethene ($C_2H_4N_4O_4$), also known as DADNE or FOX-7 (Fig. 1a).¹⁰⁻¹² FOX-7 was chosen as a representative IHE crystal because of its low sensitivity to shock initiation, relative to conventional HEs such as RDX and cyclotetramethylene tetranitramine (HMX),¹¹ and because FOX-7 single crystals can be grown to sizes suitable for plate impact experiments (in contrast to many other IHEs). FOX-7 crystallizes in a monoclinic structure (α phase, $P2_1/n$ space group), with the molecules forming wave-shaped layers having extensive intra- and inter-molecular hydrogen bonding within the layers (Fig. 1b).¹² Static compression experiments¹³⁻¹⁷ have shown that FOX-7 undergoes structural phase transformations to another monoclinic structure (α' phase) at 2 GPa and to a triclinic structure (ε phase) at 4.5 GPa; the volume change associated with these transformations is small.¹⁷ The comprehensive static pressure data by Dreger and co-workers^{13,15-17} on FOX-7 single crystals provide an excellent foundation for shock compression studies.

The objectives of this study were: (i) to determine the shock compression response of FOX-7 single crystals, including the stress threshold for shock-induced chemical decomposition,

and (ii) to develop a material description for shocked FOX-7 single crystals. To address these two objectives, plate impact experiments were conducted to measure wave profiles in FOX-7 single crystals shocked up to 21 GPa. The experimental results were analyzed using well-established shock wave analysis methods¹⁸⁻¹⁹ and also using numerical simulations. The methods used in the plate impact experiments are described next.

II. EXPERIMENTAL METHODS

FOX-7 starting material was obtained as a fine powder from Dr. Joel R. Carney of the Naval Surface Warfare Center–Indian Head Division (NSWC-IHD). Single crystals were grown from a solution of FOX-7 in dimethyl sulfoxide (DMSO) by slow evaporation at room temperature.¹³ The single crystals were cleaved parallel to the {101} plane (i.e. the *ac* plane in Fig. 1b) and polished to obtain samples having 1 – 2 mm lateral dimensions and thicknesses ranging from ~130 – 260 μ m. Because the FOX-7 single crystals are extremely fragile, considerable care was required in sample preparation. The cleaved and polished single crystals having {101} faces were bonded to a 1050 Al or z-cut quartz buffer and a LiF back window using epoxy. Prior to bonding, an Al mirror was deposited on the sample side of the LiF window.

The plate impact experiments were carried out using the configuration shown schematically in Fig. 2. Using powder guns having 5.2 mm or 30 mm bore diameter, C101 Cu or 6061-T651 Al flyers were impacted onto the buffer/FOX-7/LiF target assemblies. The experimental parameters, including the measured impact velocities, are listed in Table I.

Particle velocity histories were measured at the FOX-7/LiF interface using a velocity interferometer system (VISAR).²⁰ In addition, velocity histories were measured at three locations at the back of the buffer to enable determination of the shock wave arrival at the buffer/FOX-7 interface.

III. RESULTS

Six plate impact experiments were conducted for FOX-7 single crystals shocked along the *b*-axis (i.e. normal to the {101} crystal plane) to stresses ranging from 2.4 GPa to 21.4 GPa (see Fig. 1b). Because the *b*-axis is the two-fold rotation axis of the monoclinic unit cell, pure longitudinal waves resulting in uniaxial strain can be propagated along this direction.²¹ Although shock compression of FOX-7 single crystals along different orientations – similar to previous studies²⁻⁹ on conventional HE single crystals – is desirable, the layered crystal structure of FOX-7 poses significant challenges regarding sample preparation and only one crystal orientation (the *b*-axis) was examined in the experiments presented here.

The measured wave profiles at the FOX-7/LiF interface are shown in Fig. 3. Note that the time axis in Fig. 3 is normalized by the FOX-7 sample thickness to better compare the measured profiles. The profiles at stresses less than 3.8 GPa show a two-wave structure, corresponding to an elastic-inelastic shock compression response. At higher stresses, single (overdriven) waves are observed. The measured profiles show no clear indications of time-dependent response.

Shock wave velocities in the FOX-7 samples were determined from the measured shock wave arrival times at the buffer/FOX-7 and FOX-7/LiF interfaces. The measured shock velocities are listed in Table II.

IV. ANALYSIS AND DISCUSSION

A. Hugoniot states

To determine the continuum response (particle velocity, longitudinal stress, and density) in the shocked FOX-7 sample, the following procedure was used. First, the impact state in the buffer was determined using the known Hugoniot curves of the impactor^{22,23} and the buffer,^{24,25} together with the measured impact velocity. Then, the state achieved by the transmitted shock in the FOX-7 sample was determined by impedance matching¹⁸ using the buffer Hugoniot curve and the measured FOX-7 shock velocity. For the lowest stress experiment (Expt. #1), a two-step wave analysis – similar to that used previously¹⁹ – was used to determine the elastic compression state and the peak state in the shocked FOX-7 crystal. The continuum results for shocked FOX-7 determined for each experiment are shown in Table II.

Figure 4 shows the results from Table II (Expts. 2 – 6) in the shock velocity (U_S) – particle velocity (u_p) plane and the longitudinal stress (P_x) – volume (V) plane. As shown in Fig. 4(a), a linear $U_S - u_p$ relationship provides a good fit to the data.

For comparison, Fig. 4(b) also shows the $P_x - V$ curve for PETN single crystals determined from the $U_S - u_p$ relationship reported previously.⁵ The PETN curve is limited to stresses below 4 GPa because shocked PETN indicated chemical decomposition at higher stresses.⁵ Figure 4(b) shows that the Hugoniot curve of FOX-7 at lower stresses does not differ significantly from that of PETN, and is likely representative of soft molecular crystals.

B. Material Model and Numerical Simulations

To further analyze the measured wave profiles, numerical simulations were carried out using a one-dimensional wave propagation code²⁶ that utilizes the usual finite-difference, artificial viscosity approach.²⁷ The FOX-7 single crystals were described using a modeling approach strictly applicable for isotropic solids. We incorporated the usual separation of the mechanical response into the mean stress response and the deviatoric stress response.²⁷ Phenomenological models for the mean stress and deviatoric stress responses were developed to provide the correct longitudinal stress–density response for the FOX-7 single crystals.

The mean stress curve for shocked FOX-7 was determined from the linear fit to the $U_S - u_p$ Hugoniot data (Fig. 4):

$$U_S = 2.63 + 1.84u_p . \quad (1)$$

The y-intercept of the above linear fit corresponds to an ambient isentropic bulk modulus (B_S) of 13.0 GPa, which is consistent with that expected based on previous isothermal compression data.¹⁷ B_S was used, together with published thermodynamic data,^{28,29} to determine the Grüneisen parameter: $\Gamma = 1.0$.

To determine the deviatoric stress response, the shear modulus was assumed to be constant ($G = 7.5$ GPa) and shear strength was described using a von Mises-type yield stress model³⁰ that incorporated loss of strength (strain-softening behavior), with the yield stress given by

$$Y = Y_0 - M \bar{\varepsilon}_p . \quad (2)$$

In Eq. (2), $\bar{\varepsilon}_p$ is the effective inelastic strain, M is the strain-softening modulus, and Y_0 is the yield stress at the elastic limit.

Calculated wave profiles, determined using the above model, are shown together with the measured profiles in Fig. 5; experiments reaching high stresses are shown in Fig. 5(a), while those reaching lower stresses are shown in Fig. 5(b). The red solid curves were calculated using $Y_0 = 0.62$ GPa and $M = 0$, corresponding to an elastic-perfectly plastic response. The green solid curves were calculated using $Y_0 = 0.62$ GPa and $M = 5$ GPa, corresponding to a strain-softening response. The results in Fig. 5 show that, although both models provide a good match to the wave profiles measured at high stresses, the strain-softening model provides a significantly better match at low stresses.

C. Discussion

The wave profiles for shocked FOX-7, shown in Fig. 3, show features typical of an elastic-inelastic response to shock wave compression. No features suggestive of shock-induced structural phase transformation were observed, as expected based on the small volume changes determined previously for the known transformations.¹⁷ In addition, no signs of energy release due to shock-induced chemical decomposition were observed in the measured wave profiles (Fig. 3) or in the Hugoniot curves (Fig. 4). Therefore, the results presented here show that FOX-7 single crystals do not undergo detectable energy release – due to chemical decomposition – under shock compression to at least 21 GPa. In contrast, shocked PETN – a conventional HE – showed clear indications of chemical decomposition at shock stresses as low as 4 GPa.⁵ Thus, the present results have provided the first demonstration of the insensitivity of an IHE single crystal under plane shock compression.

The wave profiles shown in Fig. 3 show no clear indications of a time-dependent response and wave profiles calculated using a time-independent material model provide a good match to all the measured profiles, as shown in Fig. 5. The calculated profiles in Fig. 5 also show that shocked FOX-7 undergoes a loss of strength under shock wave compression.

In Fig. 6, the measured FOX-7 profile from Expt. 1 is compared with wave profiles measured previously⁴ for PETN single crystals shocked along the [100] and [110] orientations – crystal orientations determined to be insensitive and sensitive to shock-induced chemical decomposition, respectively.^{2,3} The elastic wave amplitudes and peak stresses for shocked PETN, determined from numerical simulations,³¹ are shown in the figure. Unlike the present FOX-7 profiles, which were measured using LiF windows, the PETN profiles were measured using PMMA windows,⁴ resulting in significantly larger measured sample/window interface velocities. Hence, the PETN profiles in Fig. 6 reach similar interface velocities compared to the FOX-7 profile, despite the peak stresses being lower by a factor of two.

Figure 6 shows that the elastic wave amplitude determined for shocked FOX-7 is comparable to that for [110] PETN (sensitive orientation) and is more than twice as large as that for [100] PETN (insensitive orientation). In addition, previous numerical simulations revealed significant loss of strength for [110] PETN, but not for [100] PETN.³¹ The large elastic wave amplitude and loss of strength in shocked [110] PETN have been associated with hindered shear and increased sensitivity to chemical decomposition.^{4,31} In contrast, the results presented here show that large elastic wave amplitudes and strength loss in shock-compressed FOX-7 do not contribute to sensitivity to chemical decomposition. In contrast to PETN, the underlying mechanisms for shock-induced chemical decomposition are significantly different for FOX-7.

V. Summary and Conclusions

The results presented here constitute the first reported experimental examination of the shock compression response of an IHE single crystal. These results, together with the material model and numerical simulations presented here, provide significant insight into the continuum response of shocked FOX-7 single crystals. Our main findings include:

- (1) The measured wave profiles for FOX-7 single crystals shocked to 21 GPa show no indication of energy release due to chemical decomposition. Although consistent with the expected insensitivity of FOX-7, this finding is in contrast to previous findings for conventional HEs, such as PETN, where clear indications of chemical decomposition were observed at shock stresses as low as 4 GPa.⁵

(2) At stresses below 3.8 GPa, the measured profiles and numerical simulations for FOX-7 single crystals reveal relatively large elastic wave amplitudes and significant loss of strength. Because similar features were previously associated with increased sensitivity in [110]-oriented PETN single crystals,^{4,31} the observed insensitivity of FOX-7 suggests that the underlying mechanisms for shock-induced chemical decomposition might be different.

The work on FOX-7 single crystals presented here constitutes a significant first step in addressing key scientific questions regarding the response of shocked IHEs. The wave profiles, Hugoniot curve, and phenomenological material description for shocked FOX-7 single crystals presented here provide a necessary and important foundation for future experimental and theoretical studies.

Many important scientific questions regarding FOX-7 and other IHEs remain to be answered. For example, the present experiments did not attain sufficiently high stresses to observe signs of energy release due to chemical reaction in shocked FOX-7. Therefore, wave profile measurements to stresses significantly higher than 21 GPa are needed to address the question: What is the onset stress for shock-induced chemical decomposition on FOX-7 single crystals? In addition, because continuum measurements – such as determination of wave profiles – are not sensitive to the early stages of chemical reaction before the onset of significant energy release, molecular-level measurements – such as optical spectroscopy – are needed to provide a more sensitive determination of the chemical decomposition onset stress. Also, continuum measurements alone cannot provide direct insight into the following fundamental scientific question: Why are IHEs insensitive to shock initiation? Effectively addressing this and other fundamental questions regarding IHEs will require both molecular-level measurements and theoretical calculations.

Acknowledgements

N. Arganbright is acknowledged for his expert help with the preparation of the FOX-7 single crystals. The FOX-7 single crystals were grown by Z. Dreger and N. Arganbright. K. Zimmerman, J. Friedman, and T. Eldredge are acknowledged for their assistance with the plate

This is the author's peer reviewed, accepted manuscript. However, the online version of record will be different from this version once it has been copyedited and typeset.

PLEASE CITE THIS ARTICLE AS DOI: 10.1063/1.5140194

impact experiments. This work was supported by the Office of Naval Research Grant N00014-16-1-2088 and the Department of Energy/National Nuclear Security Administration Cooperative Agreement DE-NA0002007.

References

- ¹ P. R. Lee, in *Explosives Effects and Applications*, edited by J. A. Zukas and W. P. Walters (Springer, New York, 1998), p. 259. See also: Proceedings of the International Detonation Symposium (Office of Naval Research, Arlington, 2010, 2014, 2018).
- ² J. J. Dick, *Appl. Phys. Lett.* **44**, 859 (1984).
- ³ J. J. Dick, R. N. Mulford, W. J. Spencer, D. R. Pettit, E. Garcia, and D. C. Shaw, *J. Appl. Phys.* **70**, 3572 (1991).
- ⁴ J. J. Dick and J. P. Ritchie, *J. Appl. Phys.* **76**, 2726 (1994).
- ⁵ J. J. Dick, *J. Appl. Phys.* **81**, 601 (1997).
- ⁶ J. J. Dick, D. E. Hooks, R. Menikoff, and A. R. Martinez, *J. Appl. Phys.* **96**, 374 (2004).
- ⁷ D. E. Hooks, K. J. Ramos, and A. R. Martinez, *J. Appl. Phys.* **100**, 024908 (2006); see also the erratum: *J. Appl. Phys.* **109**, 089901 (2011).
- ⁸ M. J. Cawkwell, K. J. Ramos, D. E. Hooks, and T. D. Sewell, *J. Appl. Phys.* **107**, 063512 (2010).
- ⁹ K. J. Ramos, D. E. Hooks, T. D. Sewell, and M. J. Cawkwell, *J. Appl. Phys.* **108**, 066105 (2010).
- ¹⁰ N. V. Latypov, J. Bergman, A. Langlet, U. Wellmar, and U. Bemm, *Tetrahedron* **54**, 11525 (1998).
- ¹¹ H. Östmark, A. Langlet, H. Bergman, N. Wingborg, U. Wellmar, and U. Bemm, in Proceedings of the Eleventh International Detonation Symposium, edited by J. M. Short and J. E. Kennedy (Office of Naval Research, Arlington, 1998), p. 807.
- ¹² U. Bemm and H. Östmark, *Acta Crystallogr., Sect. C: Cryst. Struct. Commun.* **54**, 1997 (1998).
- ¹³ Z. A. Dreger, Y. Tao, and Y. M. Gupta, *J. Phys. Chem. A* **118**, 5002 (2014).
- ¹⁴ S. Hunter, P. L. Coster, A. J. Davidson, D. I. A. Millar, S. F. Parker, W. G. Marshall, R. I. Smith, C. A. Morrison, and C. R. Pulham, *J. Phys. Chem. C* **119**, 2322 (2015).

- ¹⁵ Z. A. Dreger, A. I. Stash, Z.-G. Yu, Y.-S. Chen, Y. Tao, and Y. M. Gupta, *J. Phys. Chem. C* **120**, 12118 (2016).
- ¹⁶ Z. A. Dreger, Y. Tao, and Y. M. Gupta, *J. Phys. Chem. C* **120**, 11092 (2016).
- ¹⁷ Z. A. Dreger, A. I. Stash, Z.-G. Yu, Y.-S. Chen, Y. Tao, and Y. M. Gupta, *J. Phys. Chem. C* **120**, 27600 (2016).
- ¹⁸ J. M. Walsh, M. H. Rice, R. G. McQueen, and F. L. Yarger, *Phys. Rev.* **108**, 196 (1957).
- ¹⁹ S. J. Turneaure, J. M. Winey, and Y. M. Gupta, *J. Appl. Phys.* **100**, 063522 (2006).
- ²⁰ L. M. Barker and R. E. Hollenbach, *J. Appl. Phys.* **43**, 4669 (1972).
- ²¹ J. M. Winey and Y. M. Gupta, *J. Appl. Phys.* **96**, 1993 (2004).
- ²² LASL Shock Hugoniot Data, edited S. P. Marsh (University California Press, Berkeley, 1980).
- ²³ P. A. Rigg, M. D. Knudson, R. J. Scharff, and R. S. Hixson, *J. Appl. Phys.* **116**, 033515 (2014).
- ²⁴ S. C. Jones and Y. M. Gupta, *J. Appl. Phys.* **88**, 5671 (2000).
- ²⁵ D. Choudhuri and Y. M. Gupta, in *Shock Compression of Condensed Matter - 2011*, edited by M. L. Elert, W. T. Buttler, J. P. Borg, J. L. Jordan, and T. J. Vogler (American Institute of Physics, New York, 2012).
- ²⁶ Y. M. Gupta, COPS Wave Propagation Code (SRI International, Menlo Park, CA, 1976).
- ²⁷ M. L. Wilkins, in *Methods in Computational Physics, Vol. 3*, edited by B. Alder, S. Fernbach, and M. Rotenberg (Academic, New York, 1964), p. 211.
- ²⁸ J. Evers, T. M. Klapotke, P. Mayer, G. Oehlinger, and J. Welch, *Inorg. Chem.* **45**, 4996 (2006).
- ²⁹ Q. Sun, Y. Zhang, K. Xu, Z. Ren, J. Song, and F. Zhao, *J. Chem. Eng. Data* **60**, 2057 (2015).
- ³⁰ For example, see L. E. Malvern, *Introduction to the Mechanics of a Continuous Medium* (Prentice-Hall, New Jersey, 1969).
- ³¹ J. M. Winey and Y. M. Gupta, *J. Appl. Phys.* **107**, 103505 (2010).

Table I. Parameters for plate impact experiments on FOX-7 single crystals shocked normal to the (101) plane.

Experiment	Impactor	Buffer	FOX-7	Impact
Number			Thickness (μm)	Velocity (mm/ μs)
1 (18-UL03)	6061-T651 Al	z-cut quartz	196 ± 2	0.556 ± 0.003
2 (19-UL03)	6061-T651 Al	z-cut quartz	142 ± 2	0.772 ± 0.004
3 (17-UL05)	6061-T651 Al	1050 Al	155 ± 4	0.795 ± 0.004
4 (18-UL08)	6061-T651 Al	1050 Al	138 ± 2	1.663 ± 0.008
5 (19-601)	C101 Cu	1050 Al	256 ± 2	1.691 ± 0.008
6 (18-630)	C101 Cu	1050 Al	254 ± 2	2.185 ± 0.011

Table II. Results for FOX-7 single crystals shocked normal to the (101) plane.

Experiment	Shock	Particle	Stress	Density
Number	Velocity	Velocity	(GPa)	(g/cc)
	(mm/ μs)	(mm/ μs)		
1 (18-UL03) ^a	3.60 ± 0.11	0.145 ± 0.007	0.98 ± 0.05	1.964 ± 0.004
	$/3.15 \pm 0.11$	$/0.379 \pm 0.004$	$/2.43 \pm 0.05$	$/2.104 \pm 0.006$
2 (19-UL03)	3.56 ± 0.19	0.523 ± 0.008	3.50 ± 0.14	2.211 ± 0.025
3 (17-UL05)	3.71 ± 0.29	0.547 ± 0.013	3.82 ± 0.21	2.214 ± 0.038
4 (18-UL08)	4.55 ± 0.24	1.095 ± 0.019	9.39 ± 0.33	2.486 ± 0.054
5 (19-601)	5.42 ± 0.12	1.483 ± 0.013	15.16 ± 0.24	2.595 ± 0.030
6 (18-630)	6.07 ± 0.15	1.869 ± 0.019	21.36 ± 0.38	2.726 ± 0.041

^a For Expt. 1, continuum variables are listed for the elastic compression state/peak state of the observed two-wave structure. Also, the shock velocities shown are for the elastic wave/inelastic wave; the inelastic wave velocity has been corrected for the compression arising from the elastic wave.

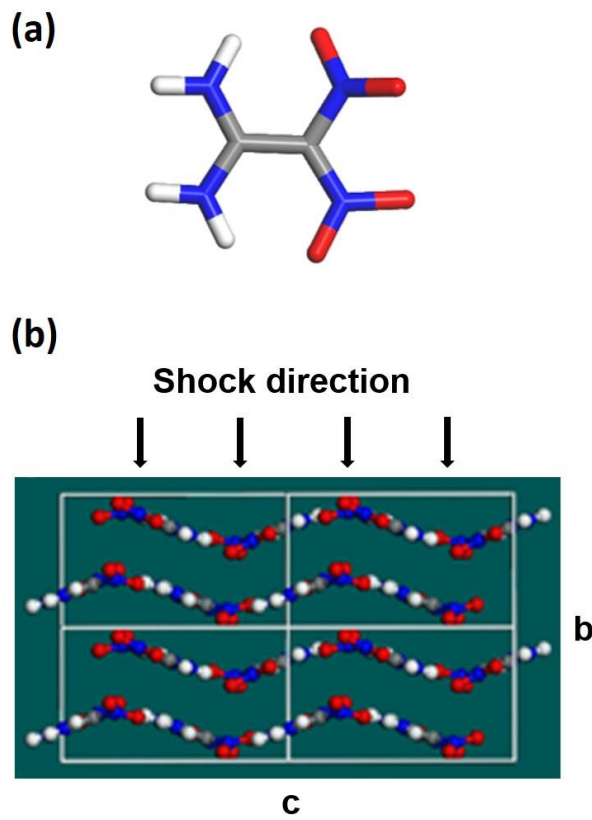


Figure 1. The FOX-7 molecule (a) and the direction of shock compression in FOX-7 single crystals (b). The crystal structure shown is a projection onto the bc plane, where b is the two-fold rotation axis of the monoclinic unit cell. Atoms are indicated by the following colors: carbon – grey; nitrogen – blue; oxygen – red; hydrogen – white. Crystal unit cells are indicated by white lines.

This is the author's peer reviewed, accepted manuscript. However, the online version of record will be different from this version once it has been copyedited and typeset.
PLEASE CITE THIS ARTICLE AS DOI: 10.1063/1.5140194

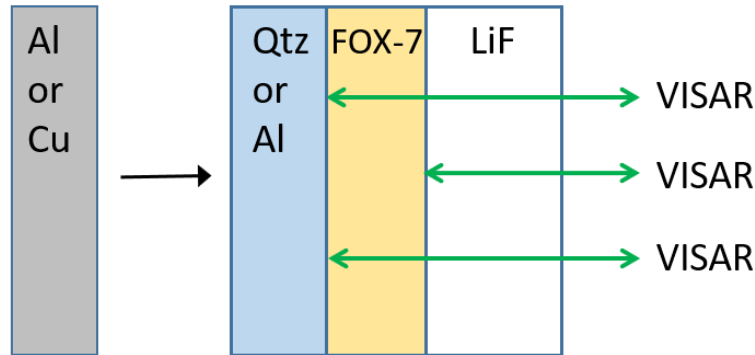


Figure 2. Experimental configuration for plate impact experiments on FOX-7 single crystals.

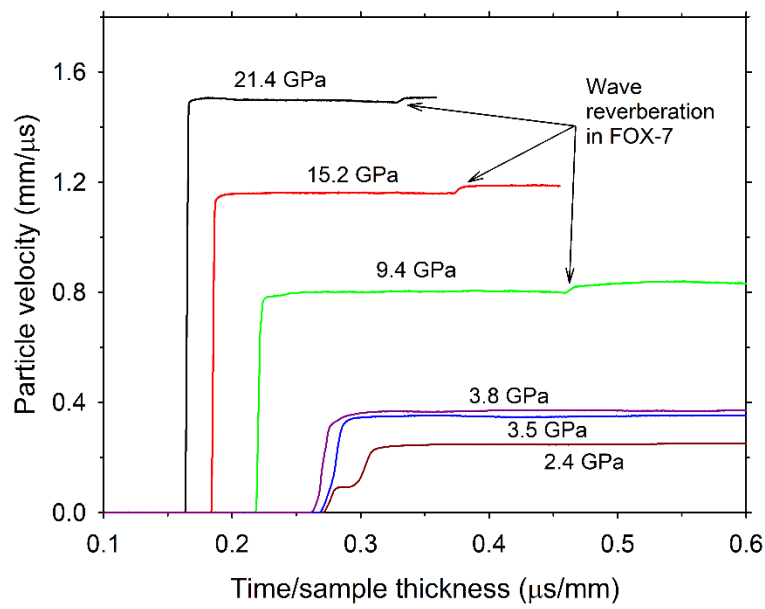


Figure 3. Measured wave profiles for shocked FOX-7 single crystals. Time is relative to shock wave arrival at the buffer/FOX-7 interface. The time axis is normalized by the FOX-7 sample thickness.

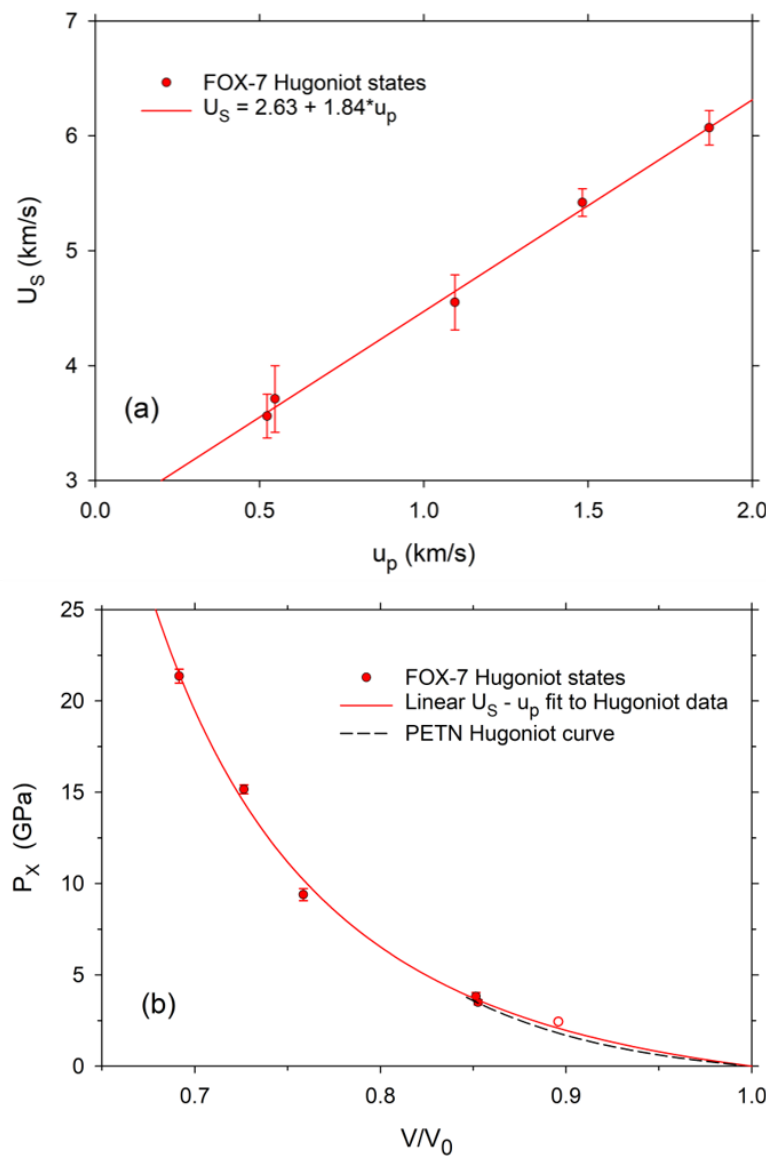


Figure 4. Measured FOX-7 Hugoniot states in the $U_S - u_p$ plane (a) and $P_x - V$ plane (b). The red solid curves are the result of a linear fit to the $U_S - u_p$ data. The red open circle (not included in the linear fit) is the peak state from Expt. 1. For comparison, the black dashed curve in (b) shows the $P_x - V$ curve for PETN single crystals (Ref. 5). The PETN curve is limited to stresses below 4 GPa because shocked PETN showed indications of chemical decomposition at higher stresses (Ref. 5).

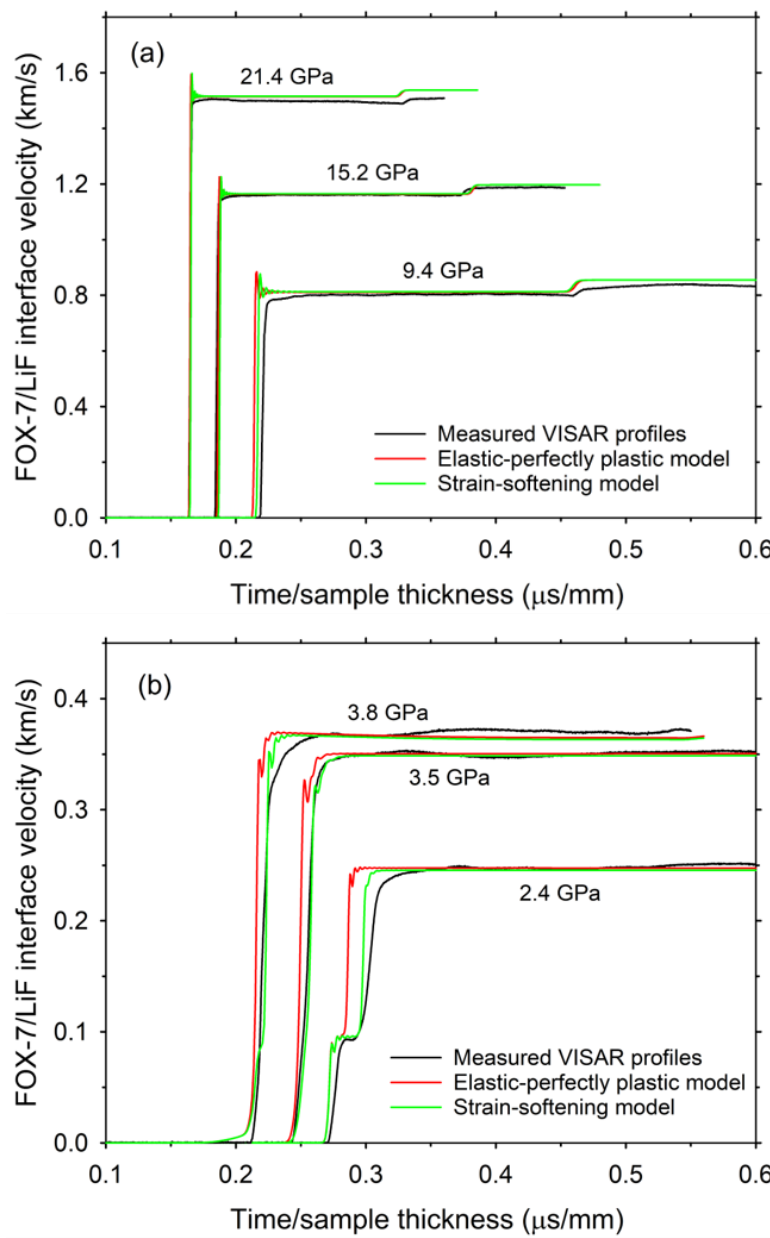


Figure 5. Calculated and measured wave profiles for FOX-7 single crystals at high stresses (a) and lower stresses (b). Time is relative to shock wave arrival at the buffer/FOX-7 interface. The time axis is normalized by the FOX-7 sample thickness. For visual clarity, the profiles for Expts. 2 and 3 are shifted 0.025 μ s/mm and 0.050 μ s/mm to the left, respectively.

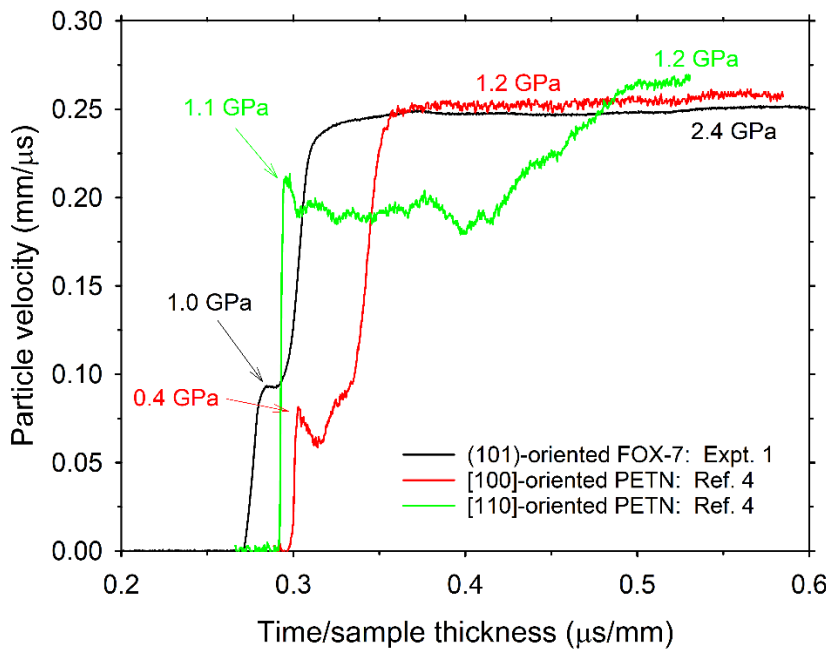
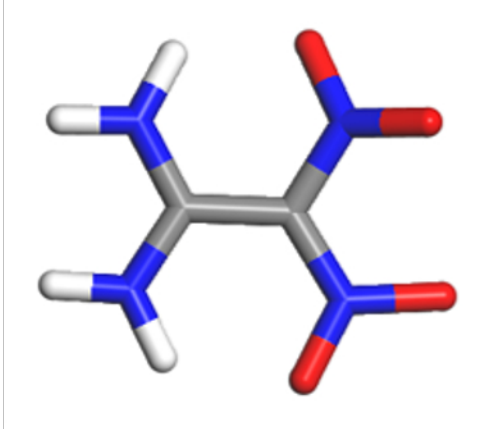


Figure 6. Measured wave profile for FOX-7 single crystal (Expt. 1), compared to measured profiles for PETN single crystals (Ref. 4). Time is relative to shock wave arrival at the buffer/sample interface; the time axis is normalized by the sample thickness. In contrast to the LiF window used in Expt. 1, the experiments in Ref. 4 incorporated a PMMA window; the PETN profiles shown here were measured at the PETN/PMMA interface. The elastic wave amplitudes and peak stresses for shocked PETN were determined from numerical simulations (Ref. 31).

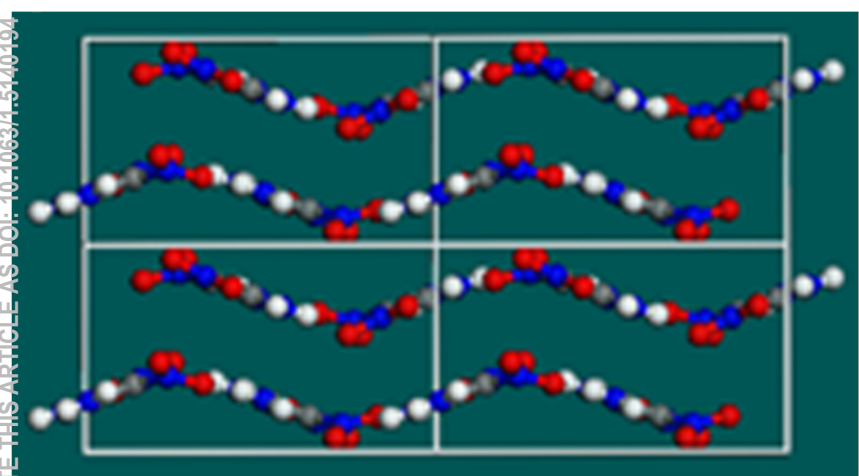
This is the author's peer reviewed, accepted manuscript. However, the online version of record will be different from this version once it has been copyedited and typeset.
PLEASE CITE THIS ARTICLE AS DOI: 10.1063/4.5140494

(a)



(b)

Shock direction

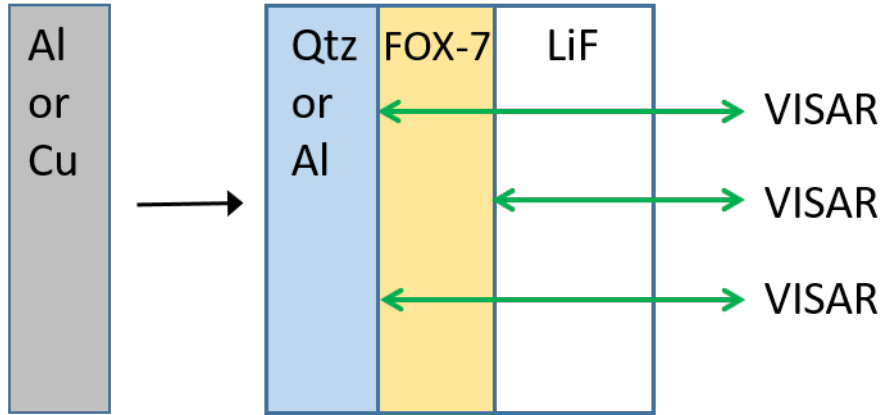


c

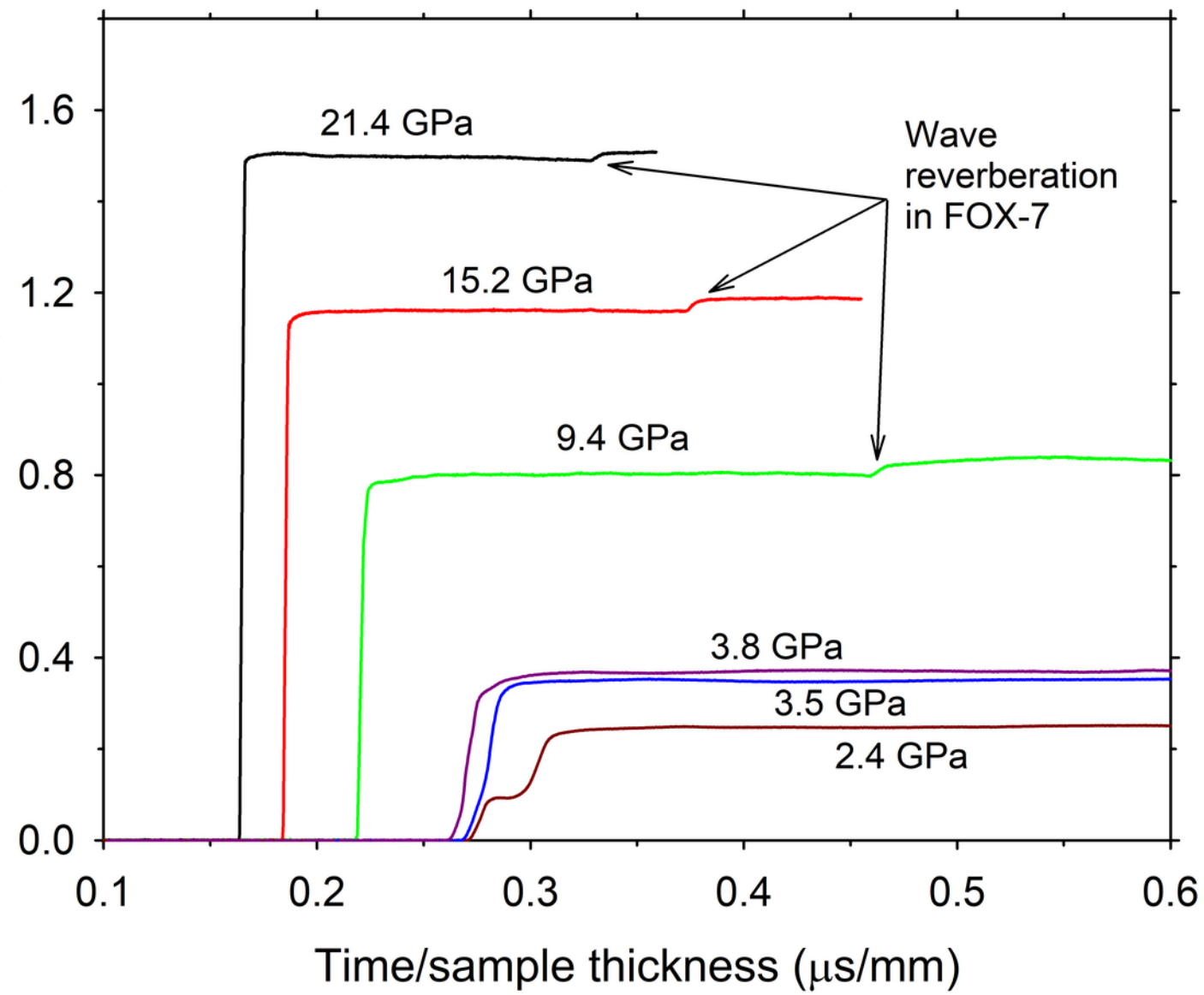
b

This is the author's peer reviewed, accepted manuscript. However, the online version of record will be different from this version once it has been copyedited and typeset.

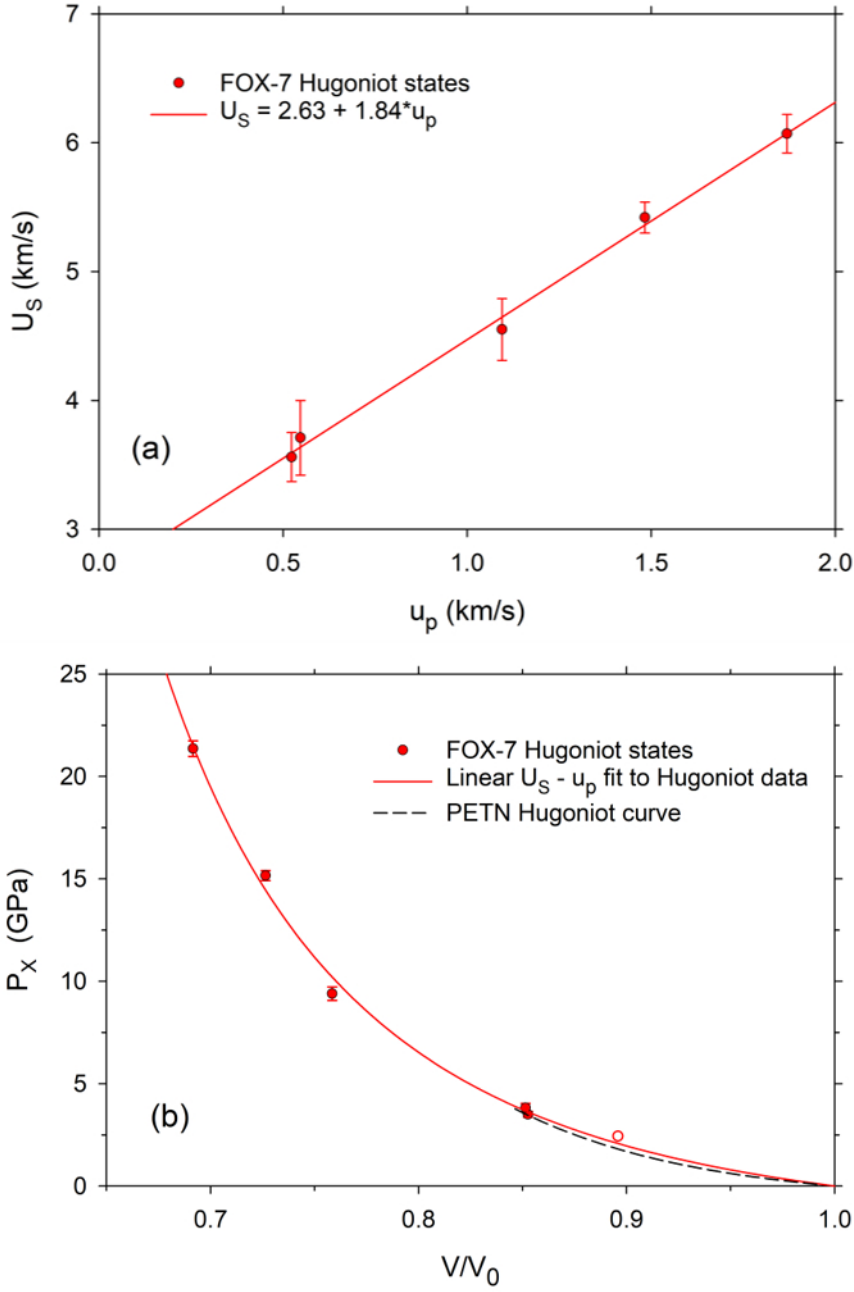
PLEASE CITE THIS ARTICLE AS DOI: 10.1063/1.5140194



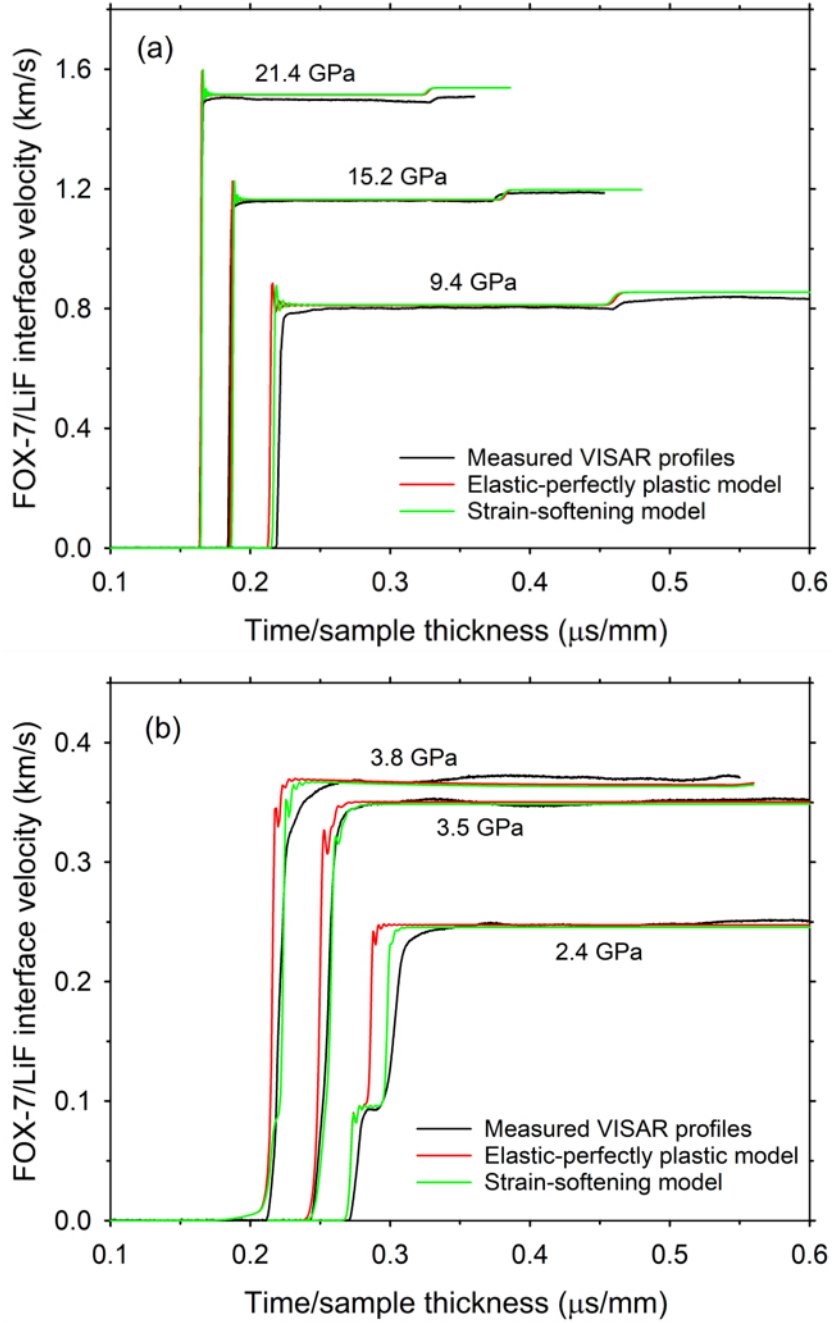
This is the author's peer reviewed, accepted manuscript. However, the online version of record will be different from this version once it has been copyedited and typeset.
PLEASE CITE THIS ARTICLE AS DOI: 10.1063/1.5150022



This is the author's peer reviewed, accepted manuscript. However, the online version of record will be different from this version once it has been copyedited and typeset.
PLEASE CITE THIS ARTICLE AS DOI: 10.1063/1.5140194



This is the author's peer reviewed, accepted manuscript. However, the online version of record will be different from this version once it has been copyedited and typeset.
PLEASE CITE THIS ARTICLE AS DOI: 10.1063/1.5140194



This is the author's peer reviewed, accepted manuscript. However, the online version of record will be different from this version once it has been copyedited and typeset.
PLEASE CITE THIS ARTICLE AS DOI: 10.1063/1.5120220

